

## Facile manipulation of individual carbon nanotubes assisted by inorganic nanoparticles†

Cite this: *Nanoscale*, 2013, 5, 6584

Rufan Zhang,<sup>‡a</sup> Zhiyuan Ning,<sup>‡b</sup> Yingying Zhang,<sup>\*c</sup> Huanhuan Xie,<sup>ac</sup> Qiang Zhang,<sup>a</sup> Weizhong Qian,<sup>a</sup> Qing Chen<sup>\*b</sup> and Fei Wei<sup>\*a</sup>

Carbon nanotubes (CNTs) are promising building blocks for nanodevices owing to their superior electrical, thermal and mechanical properties. One of the key issues for their study and application is the efficient location, transfer and manipulation of individual CNTs. In this contribution, we show that the manipulation of individual suspended CNTs has been carried out on the macroscale under low magnification, using inorganic nanoparticles (NPs) as indicators. Individual ultralong CNTs can be stretched, cut, and transferred to other substrates for further characterization. Complicated CNT structures were fabricated under optical microscopes. The inorganic NPs also facilitate the manipulation and characterization of individual CNTs under a scanning electron microscope with low magnification. Additionally, the irregular NPs deposited on suspended CNTs can also make the outer shell of the suspended CNTs display torsion or rotation around the inner shells when placed in a flow of gas, making the fabrication of CNT–NP-hybrid-based nanodevices feasible. Our results demonstrate the extraordinary capability of this manipulation technique for individual CNTs, enabled by decoration with inorganic NPs.

Received 15th April 2013

Accepted 6th May 2013

DOI: 10.1039/c3nr01877f

[www.rsc.org/nanoscale](http://www.rsc.org/nanoscale)

### Introduction

Centimeter-long carbon nanotubes (CNTs) with perfect structures have excellent properties such as high aspect ratio,<sup>1–3</sup> super strength<sup>4,5</sup> and low electrical resistivity,<sup>3,6,7</sup> rendering them promising building blocks for the next generation of micro-/nano-electronics. However, the study and application of such ultralong CNTs is highly restricted due to the difficulty in the direct location and manipulation of individual CNTs, which have macroscopic lengths but nanosized diameters. Atomic force microscopes (AFMs) have been used to directly manipulate individual CNTs on substrates. By using AFM probes, one can move, bend, stretch, roll, or twist individual CNTs, inducing various configurations or deformations on those CNTs.<sup>8–13</sup> However, the manipulation by an AFM is time-consuming, and most importantly, constrained to the microscale (typically <10 μm). In addition to AFM manipulation, transfer-printing by

polymeric mediators offers an alternative way to manipulate CNTs on surfaces and allows the fabrication of various CNT patterns.<sup>3,14,15</sup> The key to the transfer-printing technique is the choice of a suitable polymeric mediator, which determines the yield, fidelity, and controllability of the transferred CNTs. Polymers such as poly(dimethylsiloxane) (PDMS),<sup>14</sup> poly(methyl methacrylate) (PMMA)<sup>15</sup> and cellulose acetate (CA)<sup>3</sup> have been employed. After manipulation of CNTs, the polymeric films need to be removed, typically with the use of acetone vapor or by thermal treatment. However, there are always some polymeric residues left on the CNTs, influencing the performance of any resulting CNT devices. Additionally, the transfer-printing technique typically handles many CNTs at the same time, and it is not designed to locate and manipulate individual CNTs. Compared with the above methods, a scanning electron microscope (SEM) equipped with nano-manipulators permits the observation and manipulation of individual CNTs with freedom in a three-dimensional space.<sup>5,16,17</sup> However, the operation of nano-manipulators is also limited to the microscale. To explore the full potential of ultralong individual CNTs, a practical method of manipulating them in a three-dimensional, macroscopic space is desired.

Recently, we have shown that the optical visualization of individual CNTs can be realized by their decoration with TiO<sub>2</sub> NPs.<sup>4,18</sup> We further found that other inorganic NPs, such as SnO<sub>2</sub>, could also be used as markers. With the assistance of inorganic NPs, the position of individual CNTs can be easily determined under an optical microscope, even under low

<sup>a</sup>Beijing Key Laboratory of Green Chemical Reaction Engineering and Technology, Department of Chemical Engineering, Tsinghua University, Beijing, 100084, China. E-mail: wf-dce@tsinghua.edu.cn; Fax: +8610-62772051; Tel: +8610-62785464

<sup>b</sup>Key Laboratory for the Physics & Chemistry of Nanodevices, Peking University, Beijing, 100871, China. E-mail: qingchen@pku.edu.cn; Tel: +8610-62757555

<sup>c</sup>Center for Nano and Micro Mechanics, Tsinghua University, Beijing, 100084, China. E-mail: yingyingzhang@mail.tsinghua.edu.cn; Fax: +8610-62798028; Tel: +8610-62798503

† Electronic supplementary information (ESI) available. See DOI: 10.1039/c3nr01877f

‡ The two authors contributed equally to this work.

magnification, greatly facilitating their manipulation. In this contribution, we demonstrate the facile manipulation of individual ultralong CNTs enabled by their decoration with inorganic NPs, under an optical microscope or a SEM. The stretching, cutting, and transfer of individual CNTs are also shown. Complicated structures of CNTs were fabricated with the assistance of inorganic NPs. Moreover, the outer shell of the suspended CNTs could also display torsion or rotation around the inner shells, rendering them potentially useful as nanodevices.

## Results and discussion

### Deposition of inorganic NPs on suspended CNTs

Both  $\text{TiO}_2$  and  $\text{SnO}_2$  NPs can be used as markers, though here we use  $\text{SnO}_2$  as an example. Ultralong CNTs were grown on a trench-containing silicon substrate by means of chemical vapor deposition (CVD) (Fig. S1 in ESI<sup>†</sup>).<sup>2,4</sup>  $\text{SnO}_2$  NPs were deposited onto suspended individual CNTs by CVD.  $\text{SnCl}_4$ , which is a highly volatile metal halide similar to  $\text{TiCl}_4$ , was used as the precursor.<sup>18</sup> Upon contact with humid air,  $\text{SnCl}_4$  forms a misty smog of  $\text{SnO}_2$  and  $\text{HCl}$ . Upon exposure of the suspended CNTs to the smog for 3–5 s in humid air, many  $\text{SnO}_2$  NPs will be deposited on the CNTs (Fig. 1a), forming necklace-like CNT- $\text{SnO}_2$  chains (for the detailed formation mechanism of  $\text{SnO}_2$  NPs on suspended CNTs, see ESI<sup>†</sup>). The CNT segments between the  $\text{SnO}_2$  NPs are pristine tubes. Most of the spherical  $\text{SnO}_2$  NPs have diameters of 100–1000 nm, resulting in their strong scattering of visible light and rendering them easily observable under an optical microscope. Fig. 1b shows a typical optical image of a suspended CNT decorated with  $\text{SnO}_2$  NPs. Although the pristine CNTs cannot be observed directly under an optical microscope, they can easily be tracked with the indication of the visible  $\text{SnO}_2$  NPs.

### Stretching, cutting and transfer of suspended CNTs with probes

By moving a probe adhered to an individual suspended CNT, the CNT can be stretched with different strains. For example, a tungsten probe was used to manipulate a suspended CNT under an optical microscope. The tip of the probe was *ca.* 10  $\mu\text{m}$  in diameter and it could be moved precisely in the *X*, *Y*, *Z*

directions *via* high precision mechanical controls on the probe station (Fig. S2<sup>†</sup>). Once the suspended CNT was in contact with the probe, it became firmly fixed to the tip of the probe due to the van der Waals interaction between the tip and the CNT. The suspended CNT was then stretched by continuously moving the probe in one direction. The  $\text{SnO}_2$  NPs deposited on the suspended CNT enabled us to directly monitor this process. Furthermore, by fixing a force cantilever on the probe, tensile force and relative strains could be measured during the process.

Due to the high temperature required for the growth of CNTs, only a few substrates such as silicon, quartz, and sapphire *etc.* can be used to grow ultralong CNTs, which limits the application of those CNTs. Therefore, it is important to develop an effective method to transfer the CNTs from one substrate to another. We developed a direct probe-based transfer approach, avoiding the post-treatment and residue effects inherent to the printing-transfer process. As shown in Fig. 2a, there was a suspended individual CNT crossing a trench on a substrate.  $\text{SnO}_2$  NPs were then deposited onto the suspended CNT to facilitate its optical visualization. Then four probes were moved into contact with the CNT, forming two scissor-like structures (Fig. 2b), which were used to cut a CNT segment (*ca.* 200  $\mu\text{m}$ ) from the original suspended CNT. The probes were then used as two pairs of tweezers in order to transfer the cut-off CNT segment. The cut-off CNTs can then be transferred to different substrates for further characterization and measurement. For instance, the transferred CNTs can be loaded onto a silicon substrate with markers enabling Raman spectroscopy to be performed (Fig. 2c and S3<sup>†</sup> show complete Raman spectra of a transferred CNT). The  $\text{SnO}_2$  NPs make it easy to focus a Raman laser spot onto the CNTs, yet have almost no effect on the resulting Raman spectra of the CNTs (see ESI<sup>†</sup>). Additionally, the CNTs can be transferred onto a TEM grid, greatly facilitating the TEM sample preparation of individual CNTs (Fig. 2d). Finally, the transferred CNT can also be moved directly onto a Si/ $\text{SiO}_2$  substrate with metal electrodes for electrical measurement (Fig. 2e). This offers an easy and convenient method for the characterization of individual CNTs and also for

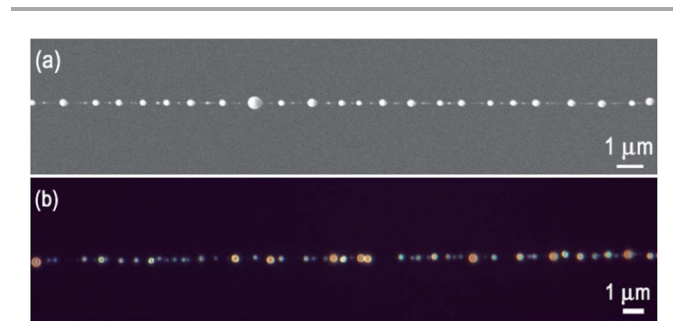


**Fig. 1** Deposition of  $\text{SnO}_2$  NPs on individual suspended CNTs. (a) SEM images of individual suspended CNTs decorated with  $\text{SnO}_2$  NPs. (b) Optical microscopy image of individual suspended CNTs decorated with  $\text{SnO}_2$  NPs.

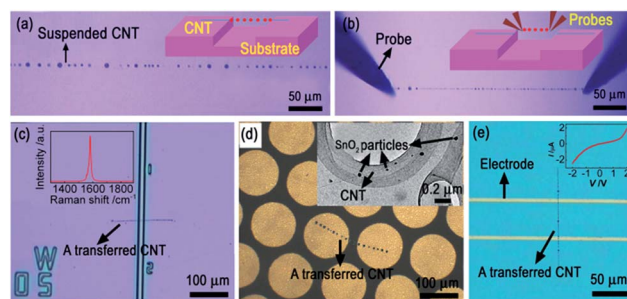


**Fig. 2** (a) Optical image of a suspended CNT decorated with nanoparticles. Inset: corresponding schematic illustration. (b) Optical image showing the cutting of a CNT segment from a suspended CNT. Inset: corresponding schematic illustration. (c) A transferred CNT segment on a substrate with markers for Raman spectroscopy. Inset: Raman spectra of the CNT shown in (c). (d) A transferred CNT segment on a TEM grid. Inset: TEM image of transferred CNT with  $\text{SnO}_2$  NPs. (e) A transferred CNT segment on a substrate with electrodes. Inset: *I*-*V* curve of a transferred CNT segment.

the fabrication of CNT devices. It should be noted that the deposition of NPs has negligible effects on the properties of CNTs (for detailed discussion, see ESI†). Moreover, the deposited SnO<sub>2</sub> NPs can be removed directly by washing with KOH solution, in order to avoid their potential influence on any subsequent characterization or synthesis (Fig. S4†).

### Fabrication of CNT structures

The probe-based CNT transfer technique can also be used to fabricate CNT structures, some typical examples of which are shown in Fig. 3. A CNT segment was cut from a suspended CNT with the use of four probes as described above. The position and orientation of the CNT segment could be easily manipulated by moving the probes, and could then be brought into contact with another suspended CNT, forming CNT cross structures (Fig. 3a and b). A knot can be made by rotating one CNT around another. More complicated two-dimensional and three-dimensional CNT structures can be fabricated in the same way, such as CNT networks (Fig. 3c and d). These CNT networks are good supports and frameworks for micro-/nano-hierarchical structures. This probe-based manipulation of individual CNTs offers a more convenient and feasible method for the fabrication of two-/three-dimensional micro-/nano-hierarchical structures, compared with conventional bottom-up approaches. Note that all of the above processes were carried out under an optical microscope, which provides an open space for the CNT manipulation.

### Manipulation of suspended CNTs in a SEM

The decoration of CNTs with SnO<sub>2</sub> NPs not only makes the manipulation of individual CNTs under optical microscopy feasible, but also facilitates the manipulation of individual CNTs in a SEM. Although SEM characterization can easily image individual CNTs grown on a substrate, it is difficult to quickly identify suspended CNTs in a SEM due to the lack of the

substrate enhancement effect.<sup>19</sup> However, for suspended CNTs decorated with SnO<sub>2</sub> NPs, it is easy to quickly find CNTs with a SEM at low magnification (Fig. 4). The suspended CNTs can be easily identified and manipulated by probes, force cantilevers, *etc.* (Fig. 4a and b). For instance, a force cantilever can be used to stretch a suspended CNT and measure its mechanical properties, such as tensile strength, breaking strain, *etc.* (Fig. 4b). SnO<sub>2</sub> NPs also play a key role in the study of inner shell sliding behavior exhibited by multi-walled CNTs (Fig. 4c–e). First, a silicon substrate with suspended CNTs was placed in a SEM equipped with nanomanipulator-based probes (Fig. S5†). The position and orientation of CNTs can be clearly determined with the assistance of SnO<sub>2</sub> NPs. A probe was moved to be in contact with the suspended CNT and the electron beam was focused on the contact part for about 30 min, depositing amorphous carbon and thus fixing the CNT onto the probe. Then the suspended CNT was stretched by moving the probe along its axial direction. In the initial stage of the stretching, the distance between all adjacent SnO<sub>2</sub> NPs gradually increased. Then the distance between two adjacent SnO<sub>2</sub> NPs increased rapidly, indicating the outer shell of the CNT had broken at a point between those two SnO<sub>2</sub> NPs. After that, the inner shell of the suspended CNT could be continuously pulled out. During the above process, the SnO<sub>2</sub> NPs (shown by a red arrow in Fig. 4d and e) deposited on the outer shell of the broken CNT remained stationary, demonstrating the ultralow friction and easy sliding between CNT shells.<sup>20–23</sup> Eventually, a millimeters-long inner tube could be completely pulled out.

### Torsion and rotation of the outer shells of suspended CNTs

The decoration of CNTs with SnO<sub>2</sub> NPs makes it feasible to observe the torsion and rotation of outer shells of suspended CNTs around the inner shells. If we deposit more SnO<sub>2</sub> NPs onto the suspended CNTs, the extra SnO<sub>2</sub> NPs form branch-like structures which are perpendicular to the suspended CNTs. If a flow of gas is introduced over the branch-like structures, the force exerted on the branches will cause the outer shells of these suspended CNTs to experience torsional force, causing them to

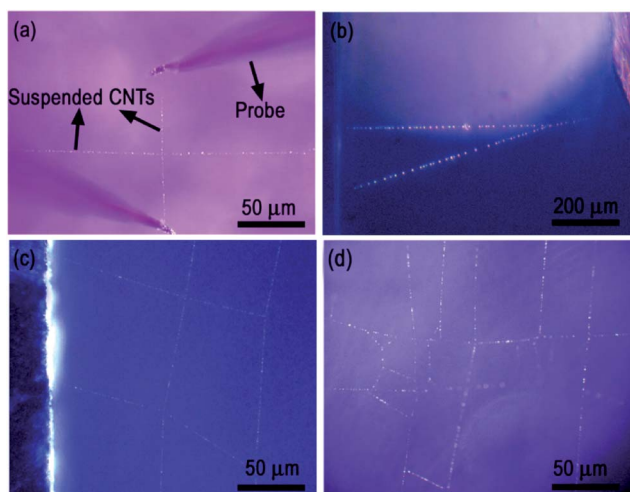


**Fig. 3** Fabrication of CNT structures. (a) Fabricating a CNT cross structure with two probes. (b) A cross structure formed by two CNTs. (c) and (d) CNT networks with different structures.

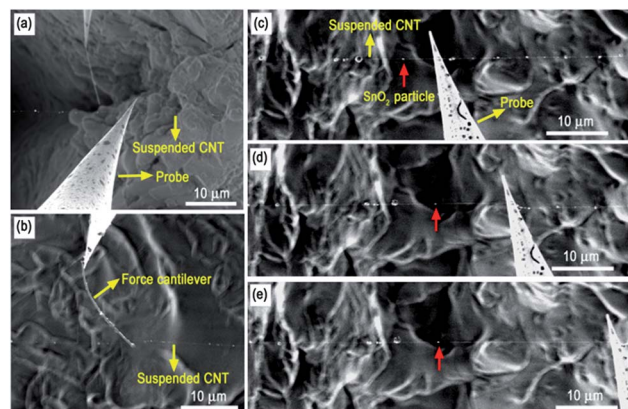


**Fig. 4** Manipulation of individual CNTs in a SEM. (a) Manipulating a suspended CNT with two probes. (b) Measuring the tensile strength of a CNT. (c)–(e) Pulling out the inner shell of a multiwalled CNT.

partially rotate around the inner shells. As shown in Fig. 5, with a gas flow exerted on the suspended CNTs, the protruding branches rotated approximately  $180^\circ$  from pointing vertically upwards to pointing vertically downwards (shown by processes (1)–(5)). This torsion is reversible, as shown in processes (5)–(9): upon removal of the gas flow, the protruding branches immediately reverted back to their initial position, pointing vertically upwards. This CNT-SnO<sub>2</sub> branch-like structure effectively demonstrates the feasibility of fabricating a micro-force sensor. In addition to the torsion of the outer shells of suspended CNTs, they were also able to rotate freely around the inner shells. As shown in Fig. 6, if the outer shell of a suspended CNT decorated with irregular SnO<sub>2</sub> NPs was cut into several shorter sections, and a gas flow was again introduced over the irregular SnO<sub>2</sub> NPs, the outer shell sections will freely rotate around the inner shell. The measured rotation speed was as high as 300–500 rpm. This interesting phenomenon demonstrates the feasibility of fabricating CNT-based nano-rotators, nano-force sensors, *etc.*

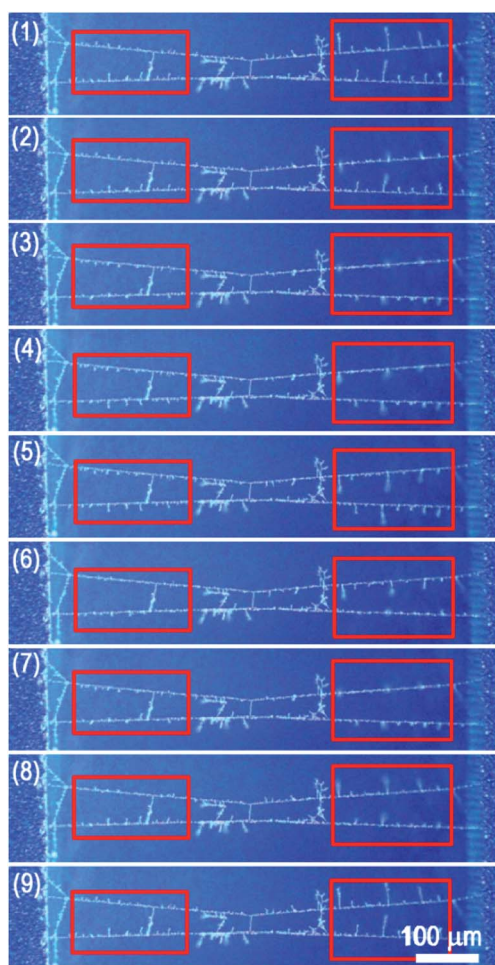


**Fig. 5** (a) Torsion-induced rotation of the outer shell of suspended CNTs decorated with SnO<sub>2</sub> NPs. The red rectangles show the outer shell sections which displayed torsion-induced rotation around the inner shell. Processes (1)–(5) show the protruding SnO<sub>2</sub> branches turning through approximately  $180^\circ$  from pointing vertically upwards to pointing vertically downwards. Processes (5)–(9) show the protruding SnO<sub>2</sub> branches returning to their initial starting position, pointing vertically upwards again.

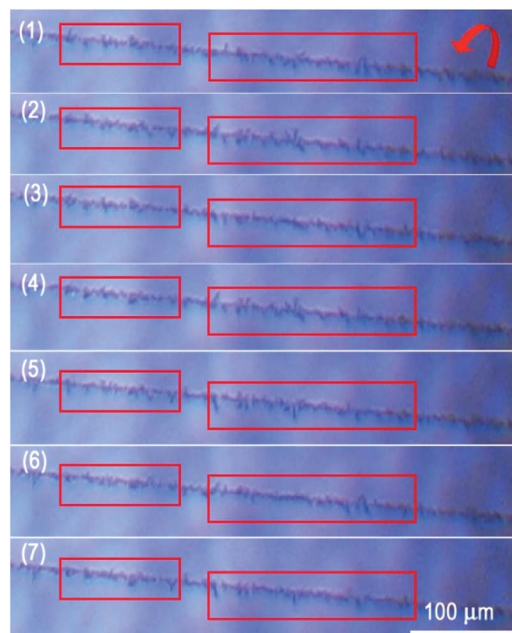


**Fig. 6** Free rotation of the outer shell of a suspended CNT decorated with SnO<sub>2</sub> NPs. (1)–(7) are snapshots from a movie recording of the fast rotation of outer shell sections decorated with irregular SnO<sub>2</sub> NPs. The red rectangles show the outer shell which was cut off from other parts and could freely rotate around the inner shell. The rotation direction is shown in the right upper corner in panel (1).

## Conclusions

In summary, a facile method for the manipulation of individual ultralong CNTs on the macroscale with the assistance of inorganic NPs was developed. The position and orientation of individual ultralong CNTs decorated with inorganic NPs could be clearly determined, making their direct manipulation feasible and convenient both under SEM and optical microscopes. Individual ultralong CNTs can be easily stretched, cut and transferred from one substrate to another for further characterization. Based on the NP-facilitated manipulation of individual CNTs, complicated CNT structures could be fabricated. Furthermore, millimeters-long tubes could be pulled out from multi-walled CNTs. With the assistance of inorganic NPs, the manipulation of individual CNTs can be easily conducted under low magnification. In addition, the CNT-NPs hybrids also make it possible to fabricate CNT-based nano-devices. The manipulation capability of individual ultralong CNTs reported here will open many possibilities for the study of mechanical properties of individual CNTs on the macroscale, and will also accelerate the development of their related applications.

## Experimental section

### Substrate preparation for the growth of CNTs

Single crystal silicon slices (10 cm long, 0.5–1 cm wide and 0.5 mm thick) were used as substrates. First, trenches (0.5–1 mm wide, 0.3–0.5 mm deep) were inscribed on the substrates by laser etching. The substrates were then cleaned with acetone,

ethanol, and deionized water in an ultrasonic bath. After that, the silicon substrates were oxidized by dry O<sub>2</sub>, wet O<sub>2</sub>, and dry O<sub>2</sub> at 1000 °C for 5, 50, and 5 min in sequence in an O<sub>2</sub> flow (500 sccm). The resulting SiO<sub>2</sub> layer on the surface had a thickness of 500 nm.

### Synthesis of ultralong CNTs

The growth of CNTs was conducted in a quartz tube (inner diameter: 31 mm). FeCl<sub>3</sub> ethanol solution (0.001–0.1 mol L<sup>-1</sup>) was used as a catalyst precursor and deposited onto substrates by a micro-printing method. After reduction in H<sub>2</sub> and Ar ( $V_{\text{H}_2} : V_{\text{Ar}} = 2 : 1$ ;  $F_{\text{total}} = 150$  sccm) at 910 °C for 15 min, the temperature was increased from 910 °C to 1000 °C over 3 min. Then CH<sub>4</sub> and H<sub>2</sub> ( $V_{\text{CH}_4} : V_{\text{H}_2} = 1 : a$ ;  $F_{\text{total}} = 80$  sccm, with 0.38% H<sub>2</sub>O) were introduced into the reactor for the growth of CNTs. The growth time was 30 min.

### Deposition of SnO<sub>2</sub> NPs on CNTs

The substrates with many CNTs on them were moved into contact with the SnCl<sub>4</sub> smog (which was spontaneously produced by the rapid hydrolysis of SnCl<sub>4</sub> in air) for the deposition of SnO<sub>2</sub> NPs. The contact time was usually 2–7 s. Contact times in excess of 15 s led to the formation of many irregular SnO<sub>2</sub> structures.

### Characterization

The CNTs were characterized by SEM (JSM 7401F, 1.0 kV; FEI, Quanta 600, 3 kV), high-resolution TEM (JEM-2010, 120.0 kV), and Raman spectroscopy (Horiba JY, 632.8 nm). The optical images were obtained with an optical microscope (long working distance metallography microscope, FS-70Z).

### Manipulation of individual CNTs using probes

An optical microscope with nanomanipulators was used to observe and manipulate individual CNTs. The substrate with suspended CNTs was placed on the stage of the optical microscope. Four probes were fixed on two pedestals on the microscope framework. The probes could be moved precisely in the X, Y and Z directions by use of high precision mechanical controls built into the pedestals. When the suspended CNTs decorated with NPs were observed with the optical microscope, the probes were moved into contact with the suspended CNTs. Then, the CNT was stretched by moving the probes in a certain direction. The deformation of the CNT could be directly monitored with the optical microscope. AFM cantilevers could also be fixed onto the probes by silver paste to measure the forces involved in the CNT manipulation.

### Removing of the SnO<sub>2</sub> NPs from CNTs

A substrate with CNTs–SnO<sub>2</sub> NPs was put into a beaker containing 20 mL KOH solution (concentration 50%), and then the solution was heated to boiling for 2 h. Upon subsequent removal of the substrate, the SnO<sub>2</sub> NPs had been completely removed from the CNTs.

## Acknowledgements

This work was supported by the Foundation for the National Basic Research Program of China (2011CB932602, 2013CB934200). and the NSF of China (60925003).

## Notes and references

- 1 R. S. Ruoff and D. C. Lorents, *Carbon*, 1995, **33**, 925–930.
- 2 Q. Wen, R. Zhang, W. Qian, Y. Wang, P. Tan, J. Nie and F. Wei, *Chem. Mater.*, 2010, **22**, 1294–1296.
- 3 Q. Wen, W. Qian, J. Nie, A. Cao, G. Ning, Y. Wang, L. Hu, Q. Zhang, J. Huang and F. Wei, *Adv. Mater.*, 2010, **22**, 1867–1871.
- 4 R. Zhang, Q. Wen, W. Qian, D. S. Su, Q. Zhang and F. Wei, *Adv. Mater.*, 2011, **23**, 3387–3391.
- 5 M. F. Yu, O. Lourie, M. J. Dyer, K. Moloni, T. F. Kelly and R. S. Ruoff, *Science*, 2000, **287**, 637–640.
- 6 X. Wang, Q. Li, J. Xie, Z. Jin, J. Wang, Y. Li, K. Jiang and S. Fan, *Nano Lett.*, 2009, **9**, 3137–3141.
- 7 Z. Liu, L. Jiao, Y. Yao, X. Xian and J. Zhang, *Adv. Mater.*, 2010, **22**, 2285–2310.
- 8 C. Thelander and L. Samuelson, *Nanotechnology*, 2002, **13**, 108–113.
- 9 P. Avouris, T. Hertel, R. Martel, T. Schmidt, H. R. Shea and R. E. Walkup, *Appl. Surf. Sci.*, 1999, **141**, 201–209.
- 10 H. W. C. Postma, A. Sellmeijer and C. Dekker, *Adv. Mater.*, 2000, **12**, 1299–1302.
- 11 T. Hertel, R. Martel and P. Avouris, *J. Phys. Chem. B*, 1998, **102**, 910–915.
- 12 B. Gao, X. Duan, J. Zhang, T. Wu, H. Son, J. Kong and Z. Liu, *Nano Lett.*, 2007, **7**, 750–753.
- 13 X. Duan, C. Tang, J. Zhang, W. Guo and Z. Liu, *Nano Lett.*, 2007, **7**, 143–148.
- 14 D. Y. Khang, J. Xiao, C. Kocabas, S. MacLaren, T. Banks, H. Jiang, Y. Y. Huang and J. A. Rogers, *Nano Lett.*, 2008, **8**, 124–130.
- 15 L. Jiao, X. Xian and Z. Liu, *J. Phys. Chem. C*, 2008, **112**, 9963–9965.
- 16 M. F. Yu, M. J. Dyer, G. D. Skidmore, H. W. Rohrs, X. K. Lu, K. D. Ausman, J. R. Von Ehr and R. S. Ruoff, *Nanotechnology*, 1999, **10**, 244–252.
- 17 B. Peng, M. Locascio, P. Zapol, S. Li, S. L. Mielke, G. C. Schatz and H. D. Espinosa, *Nat. Nanotechnol.*, 2008, **3**, 626–631.
- 18 R. Zhang, Y. Zhang, Q. Zhang, H. Xie, H. Wang, J. Nie, Q. Wen and F. Wei, *Nature Commun.*, 2013, **4**, 1727.
- 19 J. M. Bonard, K. A. Dean, B. F. Coll and C. Klinke, *Phys. Rev. Lett.*, 2002, **89**, 197602.
- 20 Q. Zheng, J. Z. Liu and Q. Jiang, *Phys. Rev. B: Condens. Matter Mater. Phys.*, 2002, **65**, 245409.
- 21 Q. Zheng and Q. Jiang, *Phys. Rev. Lett.*, 2002, **88**, 45503.
- 22 Y. Li, N. Hu, G. Yamamoto, Z. Wang, T. Hashida, H. Asanuma, C. Dong, T. Okabe, M. Arai and H. Fukunaga, *Carbon*, 2010, **48**, 2934–2940.
- 23 A. Kis, K. Jensen, S. Aloni, W. Mickelson and A. Zettl, *Phys. Rev. Lett.*, 2006, **97**, 25501.